

ACCEPTED MANUSCRIPT • OPEN ACCESS

# Mel-Frequency Cepstral and Spectral Flux Analysis of the Acoustic Signal for Real-Time Status Monitoring of Laser Cleaning

To cite this article before publication: Syafiq Ahmad Abdul Aleem *et al* 2023 *Mater. Res. Express* in press <https://doi.org/10.1088/2053-1591/acfd10>

## Manuscript version: Accepted Manuscript

Accepted Manuscript is “the version of the article accepted for publication including all changes made as a result of the peer review process, and which may also include the addition to the article by IOP Publishing of a header, an article ID, a cover sheet and/or an ‘Accepted Manuscript’ watermark, but excluding any other editing, typesetting or other changes made by IOP Publishing and/or its licensors”

This Accepted Manuscript is © 2023 The Author(s). Published by IOP Publishing Ltd.



As the Version of Record of this article is going to be / has been published on a gold open access basis under a CC BY 4.0 licence, this Accepted Manuscript is available for reuse under a CC BY 4.0 licence immediately.

Everyone is permitted to use all or part of the original content in this article, provided that they adhere to all the terms of the licence <https://creativecommons.org/licenses/by/4.0>

Although reasonable endeavours have been taken to obtain all necessary permissions from third parties to include their copyrighted content within this article, their full citation and copyright line may not be present in this Accepted Manuscript version. Before using any content from this article, please refer to the Version of Record on IOPscience once published for full citation and copyright details, as permissions may be required. All third party content is fully copyright protected and is not published on a gold open access basis under a CC BY licence, unless that is specifically stated in the figure caption in the Version of Record.

View the [article online](#) for updates and enhancements.

# Mel-Frequency Cepstral and Spectral Flux Analysis of the Acoustic Signal for Real-Time Status Monitoring of Laser Cleaning

*S.A.A. Aleem<sup>1</sup>, M. F.M Yusof<sup>2</sup>, M. Quazi<sup>3</sup>, M. A. Halil<sup>4</sup>, & M. Ishak<sup>5</sup>*

*<sup>1</sup>[sy.afiq\\_ahmad@yahoo.com](mailto:sy.afiq_ahmad@yahoo.com), <sup>2</sup>[fadhlan@ump.edu.my](mailto:fadhlan@ump.edu.my), <sup>3</sup>[moinuddin@ump.edu.my](mailto:moinuddin@ump.edu.my),  
<sup>4</sup>[aimanmh@ump.edu.my](mailto:aimanmh@ump.edu.my), <sup>5</sup>[mahadzir@ump.edu.my](mailto:mahadzir@ump.edu.my)*

*Faculty of Mechanical and Automotive Engineering Technology  
Universiti Malaysia Pahang Al-Sultan Abdullah  
Pekan, Pahang*

## ABSTRACT

Due to the fact that the laser-based cleaning process is quick, efficient, and environmentally friendly, it has been utilized in a various industry, which has increased the number of studies pertaining to this process. In addition to process optimization, the real-time monitoring system was essential in preventing the overexposure of the laser beam to the cleansed surface, which would result in an engraving effect. This article demonstrated the analysis of the acquired sound signal to identify an overexposed laser beam during laser cleaning. In order to accomplish the aim of this work, the corroded boron steel plate was prepared. The laser cleaning procedure involved a four-loop laser scan. Variable scanning speeds between 100 and 1,000 mm/s were configured. Concurrently, the acoustic signal within the frequency range of 20 Hz to 10 kHz was acquired. The results indicate that the process with a scanning speed of 1000 mm/s recorded the clear surface without morphological change on the cleaned area, whereas an unacceptable deep gouge was formed during the second and third loops of the process with speeds of 100 mm/s and 300 mm/s, respectively. According to an analysis of the acquired sound signal, the trend of the Mel Frequency Cepstral Coefficient (MFCC) was indicative of the existence of the ablated corroded substrate. In addition, the spectral flux can provide important information regarding the formation of a deep groove on a cleansed surface. This research demonstrates the feasibility of using the auditory signal to monitor the laser cleaning process. By characterizing the acoustic signal feature, it is possible to detect the completion of the cleaning process before the morphological change of the cleaned area existed. With further development, it was possible that this method would become the most efficient, resilient, and demanding in the future.

Keyword: Laser Cleaning, Real-Time Monitoring, Acoustic Method

## INTRODUCTION

In response to the expanding demand for rust, paint, and contaminant removal technology in a variety of industries, the number of innovations in this field has increased. Laser processing is one of the methods incorporated into the technology of surface cleaning. Similar to other technologies, laser cleaning also has disadvantages. Because it could affect the surface roughness of the cleaned surface, an overexposed laser beam during the cleaning process has become a significant concern. This factor becomes the disadvantage for a particular application. Accordingly, numerous studies had been conducted to determine how laser technology could be used to effectively decontaminate metallic or nonmetallic surfaces [1-2]. Despite a focus on process optimization, the need for a monitoring system for laser cleaning is undeniable, as it has also been demonstrated to be essential for attaining the desired cleaning quality [3-4].

Until recently, numerous studies had been conducted to identify a feasible real-time assessment method. In a study conducted by Xiaozhu Xie et al. [5], laser rust elimination was monitored by combining high-speed camera and structure-borne acoustic emission technology. It was discovered that the RMS of the acoustic emission signal from the significant frequency band has a significant correlation with the trend of thermal damage to the substrate surface, which can be used to evaluate the cleaning quality. Lee & Watkins [6] discovered similar results, whereas the acoustic emission energy increased proportionally with the increase in laser fluence. In a different investigation, the spectroscopic method for monitoring the cleaning process of the epoxy layer on composite materials was demonstrated [3]. This study found that the light intensity at a particular wavelength was significantly correlated with the laser power, which could provide valuable information regarding the amount of substrate ablated from the surface of a composite. The same approach was also used to monitor the paint removal process [7], resulting in a similar conclusion. Tserevelakis et al. [8] demonstrated the use of photoacoustic technology to monitor the laser polishing of the stone surface. According to the study, photoacoustic signals provide enhanced detection sensitivity at high spatial resolution.

Based on previous research, it was evident that the use of an appropriate monitoring method could assess the quality and condition of the cleaning process. In addition, it aids in controlling the process to ensure that the desired quality is accomplished. In addition to the aforementioned methods, an airborne acoustic method could also be used to attain the same objective. Even though

1  
2  
3 it is not used specifically in laser cleaning applications, this method is widely used to monitor laser  
4 ablation, which is conceptually similar to laser cleaning. Huang et al. [9] investigate the acoustic  
5 characteristics of nanosecond and femtosecond ablation. As the nanosecond laser energy  
6 increased, the study revealed that the amplitude of the acoustic signal increased slowly at first,  
7 changed swiftly in the middle, and reached a plateau at the end. In the case of femtosecond laser,  
8 the amplitude of sound was consistently linear. Stefan et. al. [10] conducted a more thorough study.  
9 They discovered that the trend of acoustic amplitude differed in the cases of low and high ablation  
10 threshold.  
11  
12

13  
14  
15  
16  
17  
18 Due to a significant correlation between acoustic signal and laser ablation in the aforementioned  
19 works, this method is possible to be used to monitor the laser cleaning status. However, in order  
20 to gain deep comprehend on how the acoustic signal could detect the overexposed laser beam  
21 which significantly affect the roughness of the cleaned surface, deeper study is needed. This was  
22 due to the insignificant number of related studies in this field that was recorded in the past. Hence,  
23 this paper investigate the viability of the acoustic method in real-time laser cleaning assessment.  
24 During the laser cleaning of the rusted Boron Steel sample, the acoustic signal was recorded. In  
25 this paper, the characteristics of the signal at different loop of the laser cleaning procedure are  
26 investigated and discussed. The acoustic signal features which are sensitive to indicate the  
27 overexposed laser beam which caused the engraving effect to the cleaned surface will be revealed.  
28  
29  
30  
31  
32  
33  
34  
35  
36  
37

## 38 **METHODOLOGY**

### 39 *Experimental Method*

40  
41  
42 Boron Steel 22MnB5 was surface-grounded and deposited in an ambient room environment for  
43 ten days to serve as the specimen for this study to obtain a uniform corrosion layer on the surface  
44 of boron steel. The laser cleaning procedure was performed at 100 mm/s, 300 mm/s, and 1000  
45 mm/s with the cleaning area of 5 mm x 5 mm. The laser intensity and pulse repetition rate (PRR),  
46 was set to 40% and 20 kHz respectively. In this study, the number of loops represent the number  
47 of completed process cycle. For instance, if the number of loops was set to 2, the cleaning process  
48 will be done twice on the same spot. Specifically, the number of loops was set to 4 in this work.  
49  
50  
51  
52  
53  
54  
55  
56  
57  
58  
59  
60

This was done to investigate how the sound signal characteristic change when the process was overdone. The detail information on the parameter setup was presented in Table 1

Table 1: The parameter setting for the laser machine.

Control Variable	Constant Variable		
Speed	Frequency	Power	Process Loops/Cycle
100mm/s			
300mm/s	20 kHz	40%	4
1000mm/s			

### Signal Acquisition

During the process, a microphone was used to acquire an acoustic signal in order to analyze the capability of acoustic technology to ascertain the status of laser cleaning. The airborne acoustic signal was obtained in the frequency range of 20 Hz to 10 kHz. In this investigation, the NI 9124 Analog-to-Digital Converter was used to sample the sound's amplitude. The sampling rate was 25.6k Samples/s. In order to examine the acoustic characteristics of various process setups, the signal acquisition system was configured as shown in Figure 1. The figure indicates that a free-field microphone was placed 25 cm from the laser point.

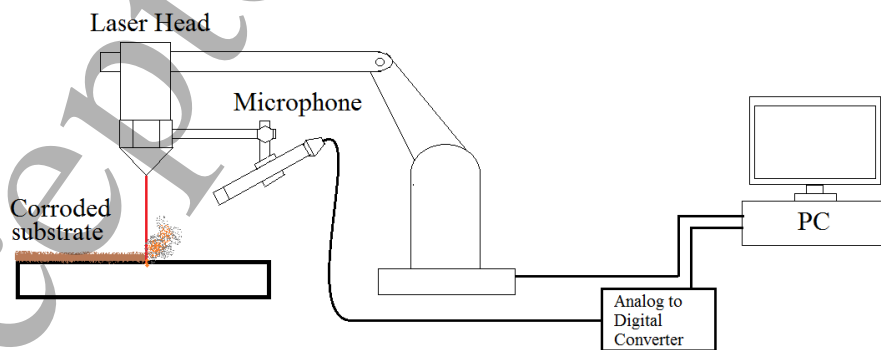


Figure 1 Signal Acquisition Setup

### *Acoustic timbre extraction*

Typically, the auditory signal is acquired as a time series. If the signal characterization includes the frequency aspect, the signal will be converted into a frequency spectrum. In previous studies, the sound signal has been quantitatively characterized to learn its correlation with the phenomenon that emerged from numerous types of process. The signals are distinguished by the trend of their timbre or characteristics.

In this study, the characteristic of the time-series sound signal will be discussed based on the variation of amplitude. After analysing the trend of the time-series sound amplitude, frequency-based characteristics were studied. In this investigation, the spectral centroid and roll-off frequency were examined to determine how they react to a change in laser cleaning status. The spectral centroid represents the centre frequency of the acquired sound signal. In contrast, the spectral roll off point refers to the frequency at which the energy level was below the threshold. This characteristic is typically employed to distinguish between the significant signal bandwidth and the background noise. The spectral centroid and roll-off point were essentially determined using Equations (1) and (2).

$$\text{Spectral Centroid} = \frac{\sum_{k=b_1}^{b_2} f_k S_k}{\sum_{k=b_1}^{b_2} S_k} \quad (1)$$

$$\text{Roll Off Point} = \sum_{k=b_1}^i |S_k| = K \sum_{k=b_1}^{b_2} S_k \quad (2)$$

Despite the frequency characteristic, the time-variability of the signal was also determined in this study to ascertain the cleaning status indicator. This was done by utilizing the Mel Frequency Cepstral Coefficient (MFCC) and Spectral Flux analysis. Conceptually, the MFCC is the short-term power spectrum of a sound as determined by the linear cosine transform of a log power spectrum on the mel scale frequency [11]. The step procedure for determining the MFCC of the signal was as depicted in Figure 2.

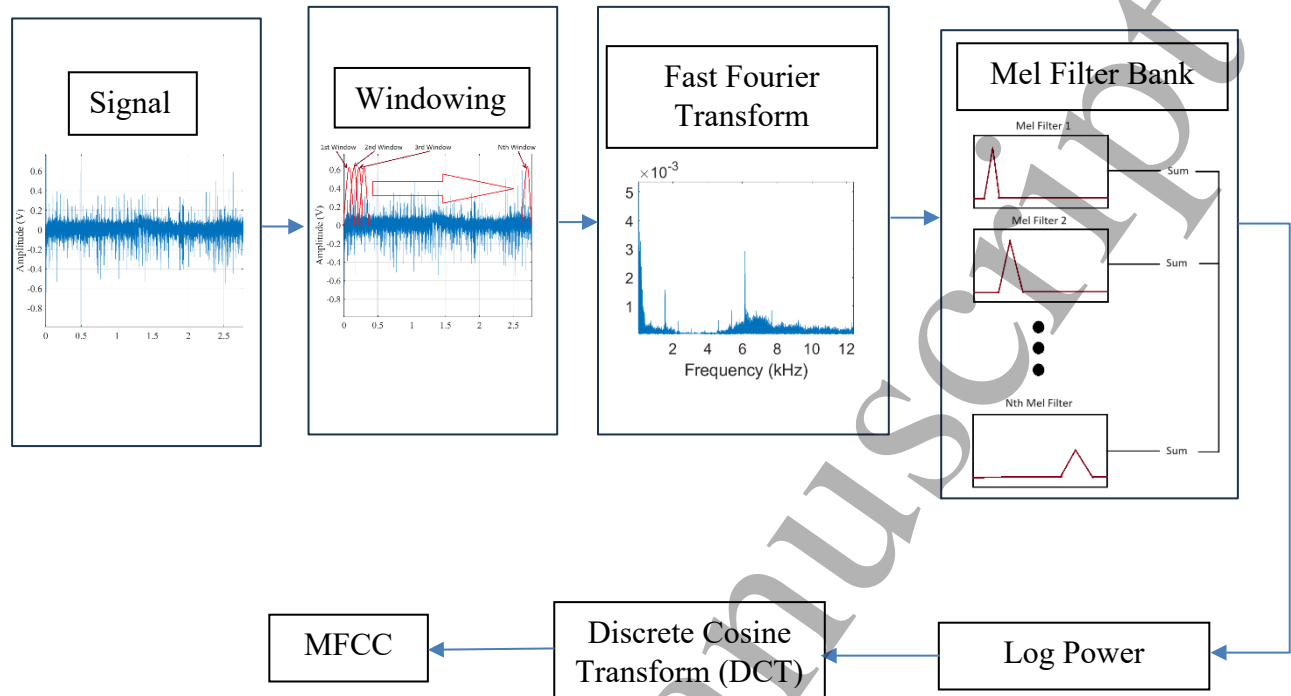


Figure 2 MFCC step procedure

The process begins with signal windowing. In this work, a hanning window was applied with 50% overlap. The signal was then transformed into a frequency spectrum using the fast fourier transform (FFT). The procedure of spectral enveloping is then accomplished by applying 10 distinct triangle mel filters. Equation 3 depicts the conversion of normal frequency to mel frequency.

$$Mel\,Freq. = 2595 \log_{10}\left(1 + \frac{f}{700}\right) \quad (3)$$

Before the discrete cosine transform (DCT) was applied to the log power signals, the log power of all mel frequencies was calculated. The MFCC was determined using equation 4, where  $c_i$ ,  $N_f$ ,  $S_n$ , and  $N$  represent the  $i_{th}$  MFCC coefficient, the number of triangular filters, the log energy output of the  $N_{th}$  filter coefficient, and the number of MFCC.

$$c_i = \sum_{n=1}^{N_f} S_n \cos \left[ i(n - 0.5) \left( \frac{\pi}{N_f} \right) \right], \quad i = 1, 2, 3, \dots, N \quad (4)$$

In contrast, the spectral flux of the signal was calculated using equation 5.  $S_k$  represents the spectral value at bin  $k$  in this equation. Meanwhile,  $B_1$  and  $b_2$  are the band boundaries, whereas  $P$  is the norm type.

$$Flux(t) = \left( \sum_{k=b_1}^{b_2} |S_k(t) - S_k(t-1)|^P \right)^{\frac{1}{P}} \quad (5)$$

## RESULTS & DISCUSSION

### *Effect of laser scanning speed to the cleaning process quality.*

Figures 3 to 5 depict the Boron Steel 22MnB5 plate surface following a laser cleaning procedure according to Table 1. Table 2 displays the average roughness after each scan or loop cycle has been completed. In Figure 3 and Table 2, for a scanning speed of 100 mm/s, the roughness of the cleaned area increased from 2.235  $\mu\text{m}$  after loop 1 to 7.202  $\mu\text{m}$  after the final loop of the procedure. In Figure 4, the roughness altered from 2.115  $\mu\text{m}$  to 4.287  $\mu\text{m}$  when 300 mm/s was used. In the case of a scanning speed of 1000 mm/s, the roughness was recorded as 2.082  $\mu\text{m}$  at the end of the first loop and changed to 2.243  $\mu\text{m}$  at the completion of the cleaning procedure. This is depicted in Figure 5. Based on these results, the cleaning procedure at 1000 mm/s exhibited the smallest change in surface roughness. The cross-sectional area of the cleansed surface in Figure 6 reveals that the process with a scanning speed of 1000 mm/s recorded the shallowest groove pattern, while the process with a scanning speed of 100 mm/s recorded the deepest groove.

The appearance of deep grooves on the surface after cleaning with a low laser scanning speed was caused by the increased interaction time between the laser beam and the specimen, which initiated the heat accumulation effect in the targeted laser cleaning areas. Consequently, there was a high temperature and energy density on the laser cleaning areas [12]. Therefore, the quantity of ablated material was not limited to the corroded layer alone, but also included the base metal, which forming a deep groove on the cleaned surface.



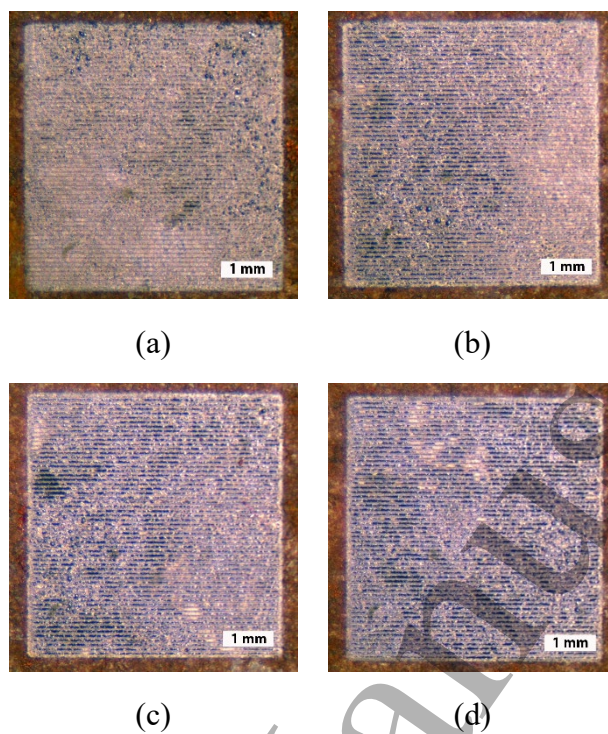


Figure 3 Cleaned area during the laser cleaning process with speed of 100 mm/s (a) 1<sup>st</sup> Loop (b) 2<sup>nd</sup> Loop (c) 3<sup>rd</sup> Loop (d) 4<sup>th</sup> Loop

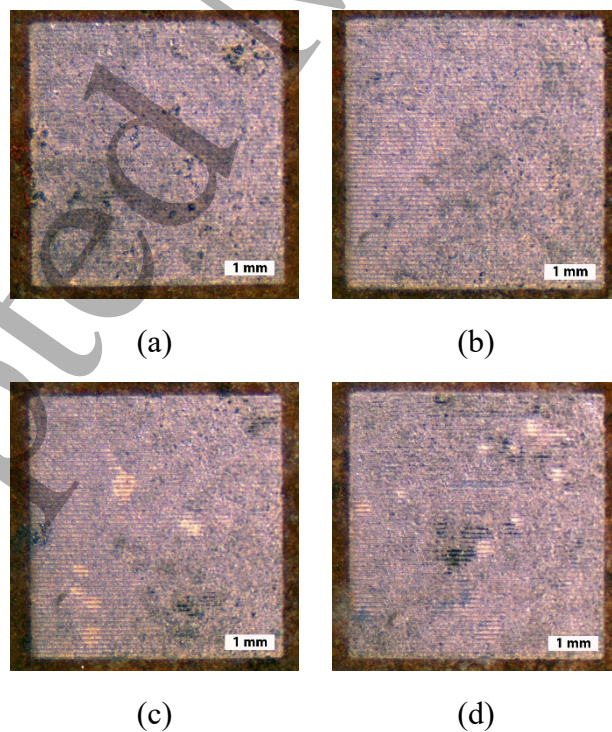


Figure 4 Cleaned area during the laser cleaning process with speed of 300 mm/s (a) 1<sup>st</sup> Loop (b) 2<sup>nd</sup> Loop (c) 3<sup>rd</sup> Loop (d) 4<sup>th</sup> Loop

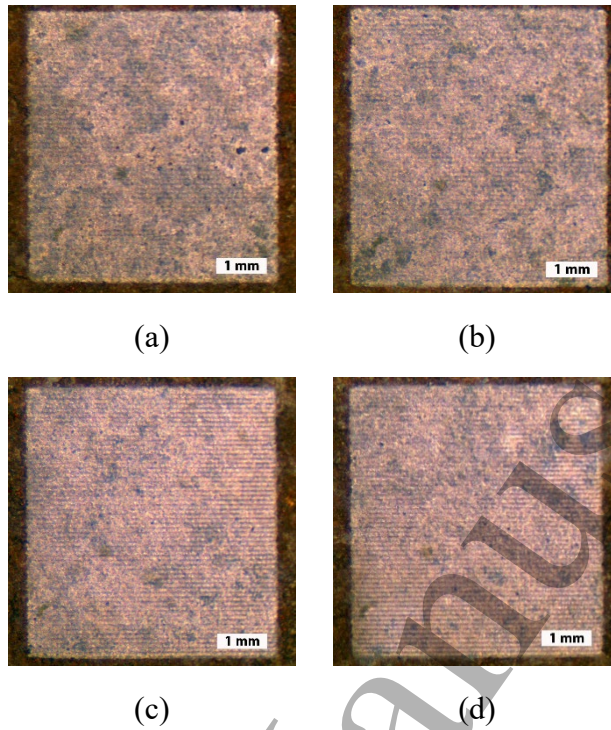


Figure 5 Cleaned area during the laser cleaning process with speed of 1000 mm/s (a) 1<sup>st</sup> Loop (b) 2<sup>nd</sup> Loop (c) 3<sup>rd</sup> Loop (d) 4<sup>th</sup> Loop

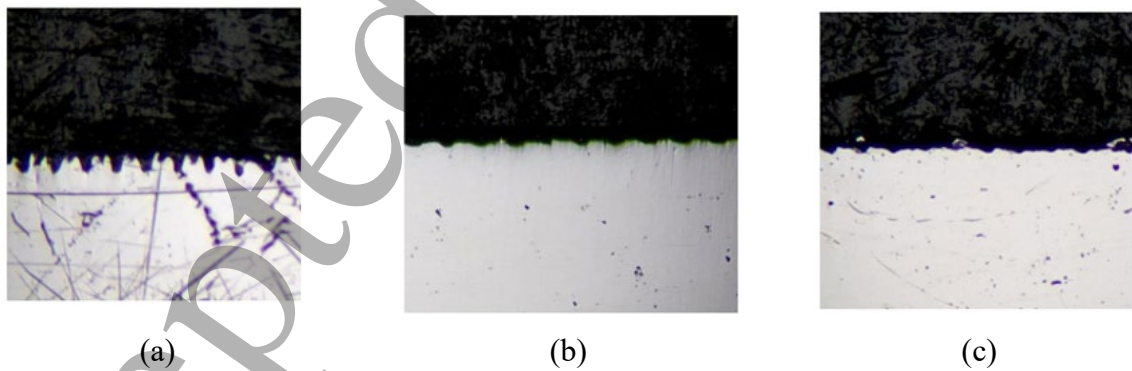


Figure 6 The groove of laser cleaning with scanning speed of (a) 100mm/s, (b) 300mm/s and (c) 1000mm/s.

After the cleaning process, it is possible to conclude that all processes contribute to the formation of the groovy surface. According to the source, it was extremely challenging to guarantee that the surface roughness returned to normal after cleaning. However, the surface roughness tolerance was considered at  $2.5\mu\text{m}$  for this study due to the lowest groovy surface as shown in Figure 6. Based on

the information in Table 2, it is possible to conclude that the cleaning process with 100 mm/s scan speed actually ended after the first loop, whereas the process with 300 mm/s scan speed ended after the second loop. In contrast, the cleaning procedure with a speed of 1000 mm/s was only completed at the final loop of the process.

The uncorroded surface's roughness was measured and compared to the surface's roughness after the completion of each laser cleaning loop in order to determine how much the surface's roughness had changed from its original state. Table 2 also displays the ratio of each loop's roughness to its initial roughness. Since the surface roughness after cleaning should not exceed approximately 2.5  $\mu\text{m}$ , the roughness ratio should not exceed 7.33 to indicate that the cleaning procedure had little impact on the surface of the cleaned area.

Table 2 Roughness After Each Laser Scan Loop

Roughness Before Corrosion ( $\mu\text{m}$ )	Roughness After Corrosion ( $\mu\text{m}$ )	Speed (mm/s)	Loop 1		Loop 2		Loop 3		Loop 4	
			Roughness ( $\mu\text{m}$ )	Ratio	Roughness ( $\mu\text{m}$ )	Ratio	Roughness ( $\mu\text{m}$ )	Ratio	Roughness ( $\mu\text{m}$ )	Ratio
0.341	2.353	100	2.235	6.55	5.764	16.90	6.296	18.46	7.202	21.12
		300	2.115	6.20	2.651	7.77	3.688	10.82	4.287	12.57
		1000	2.082	6.11	2.112	6.19	2.198	6.45	2.243	6.58

According to the ratio in Table 2, it was evident that the 100 mm/s cleaning procedure with a high roughness ratio began in the second loop. This indicates that deep grooves have already formed after the second scanning cycle has been completed. In contrast, the formation of a deep groove began following the completion of the third scanning loop in the 300 mm/s procedure.

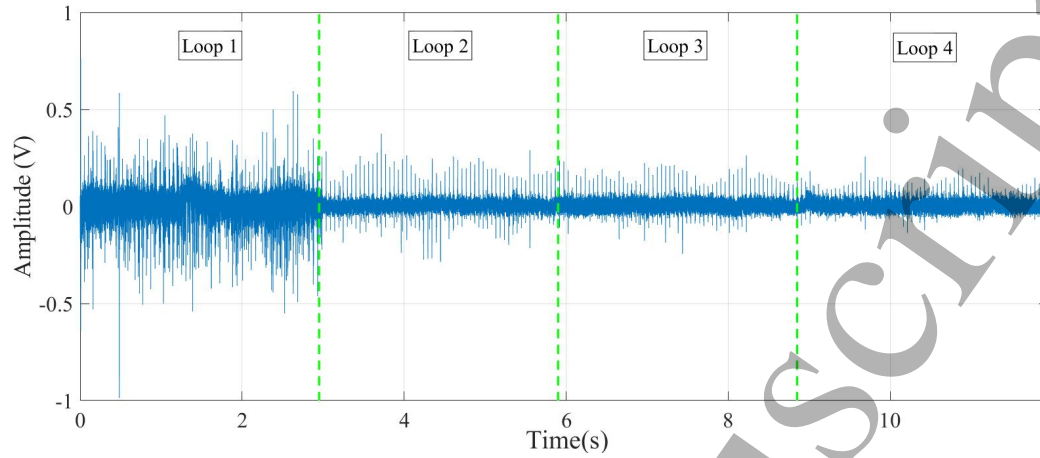
Based on these findings, it was determined that the scanning speed is the primary factor influencing the grade of laser cleaning. In some instances, the cleaning quality was poor because the cleansed surface displayed a textured groove. This occurred because the process still continued after the corroded substrate had been completely removed from the surface of the laser-cleaned area. This demonstrates the significance of having a monitoring system that could indicate the status of the process in order to prevent the process from continuing after the corroded substrate was removed, which results in the change of the surface morphology of the cleansed area.

### *Characteristic of the Acoustic Signal from laser cleaning process*

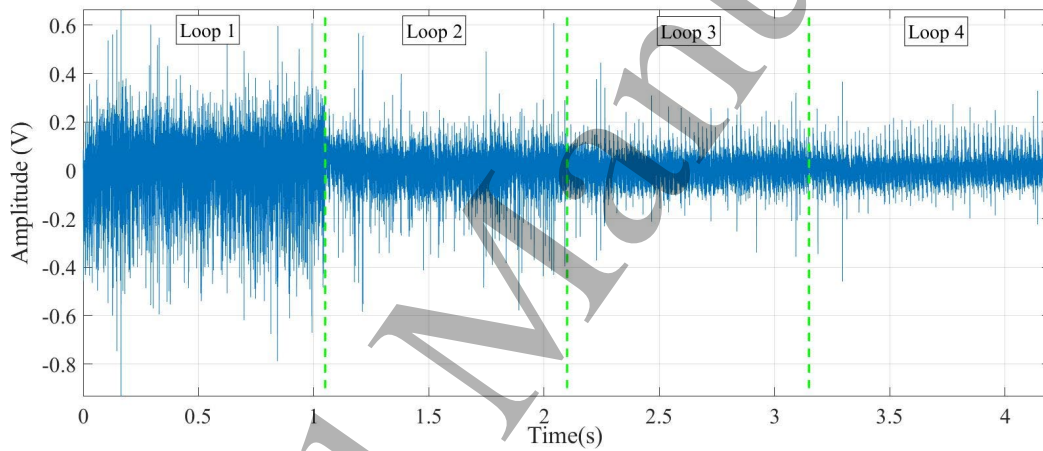
The significance of a monitoring system has been emphasized in the past, as it is necessary to indicate the end of the process to prevent the engraving effect on the cleansed surface. In this study, acoustic methods were implemented, and the audible sound signal was recorded during laser welding. As previously explained, the signal was characterized by its timbre or characteristics prior to evaluating the cleaning status information based on the trend of these characteristics.

Figure 7 depicts the signals acquired from the process using the various sets of parameters listed in Table 1. Based on Figure 7, the time needed to complete a single process loop of a laser cleaning were 2.95 s for the process with the speed of 100 mm/s. Meanwhile, the time taken to complete a single process loop was recorded to be 1.05 s for the speed of 300 mm/s. In case of the process with the speed of 1000 mm/s, the time taken to complete a single process loop was 0.38 s. As shown in Figure 7(a) and (b), during the first few seconds of the process, the sound amplitude was quite intense and exhibited an irregular pattern. This phenomenon did not manifest until 2.95 s and 2.1 s, respectively, for 100 mm/s and 300 mm/s laser scanning speeds. It occurred due to the irregular sound produced by the spark and ablation of the corroded substrate. As the process continued, increasingly regular patterns began to emerge. This can be observed in Figure 7(a) and 7(b) as the periodic amplitude appear after 2.95s and 2.1s respectively. At this point, the engraving effect depicted in Figure 6 (a) and (b) existed. During the process of engraving, the trend of ablation from the surface of the base metal had a significant impact on the sound signal pattern [10]. Due to the nature of the laser pulse, the pattern tended to be periodic, while the amplitude or energy of the signal was affected by the quantity of ablated gas ejected from the keyhole [9, 13]. In contrast, the process sound pattern with a scanning speed of 1000 mm/s in Figure 7(c) captured the irregular pattern throughout the process. From the results in Table 2, it has been determined that, based on the roughness ratio, the cleaning procedure is only complete after the fourth loop. Thus, the irregular sound pattern may have been caused by the presence of the corroded substance throughout the entire process, up until the process completion.

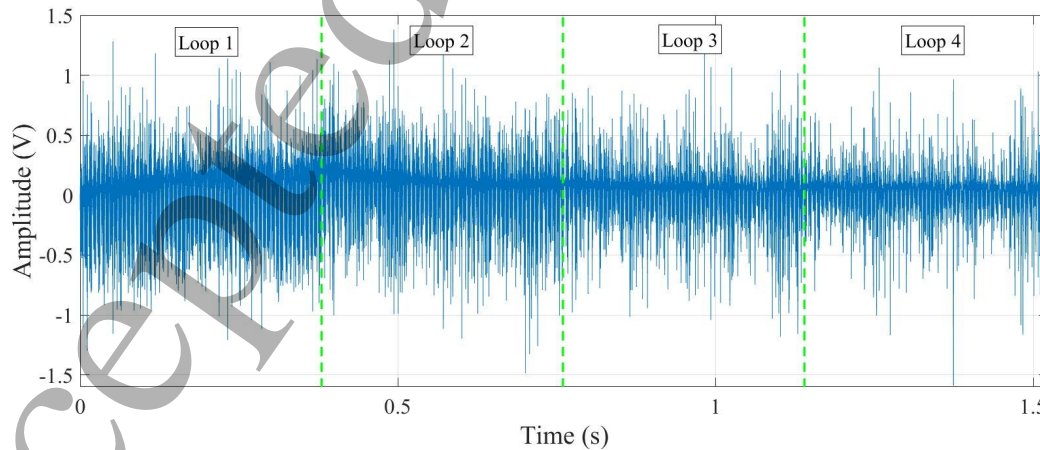




(a)



(b)

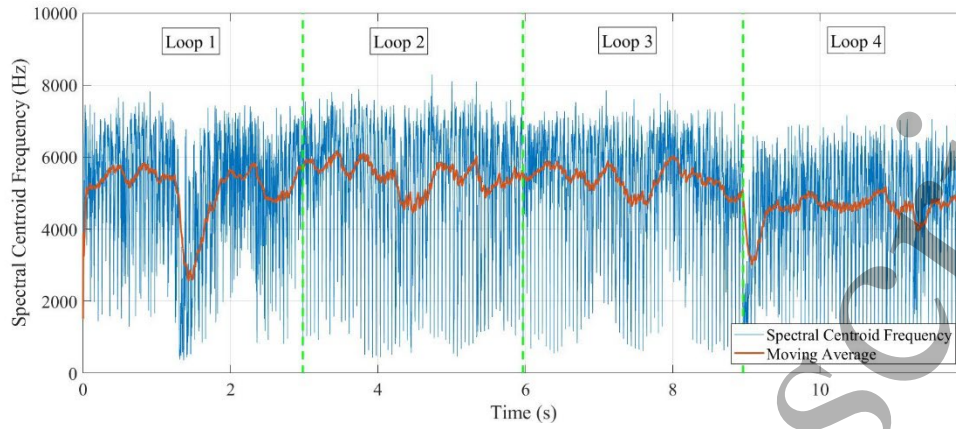


(c)

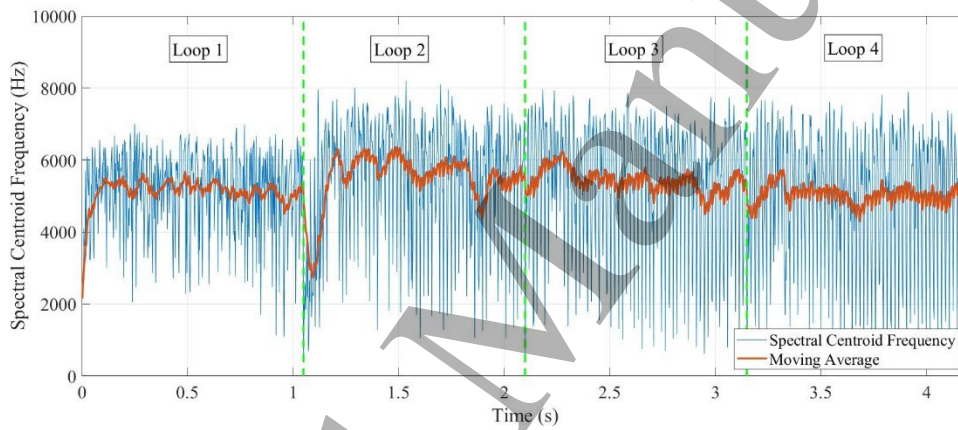
Figure 7 Characteristic of the time domain signal for a laser cleaning with different speed (a) 100 mm/s (b) 300 mm/s (c) 1000 mm/s

1  
2  
3 Based on the previously discussed results, it was determined that the time series of the sound signal  
4 could provide an in-situ trend regarding the cleaning status during the process. However, to  
5 establish a robust monitoring system, these trends must be represented quantitatively as an input  
6 of data in order for the system to function effectively. In this instance, the sound signal was  
7 typically quantified based on its characteristics or timbre. In this study, a variety of sound timbres  
8 were investigated to gain a greater understanding of the change in sound behaviour throughout the  
9 entire laser cleaning procedure.  
10  
11  
12  
13  
14  
15

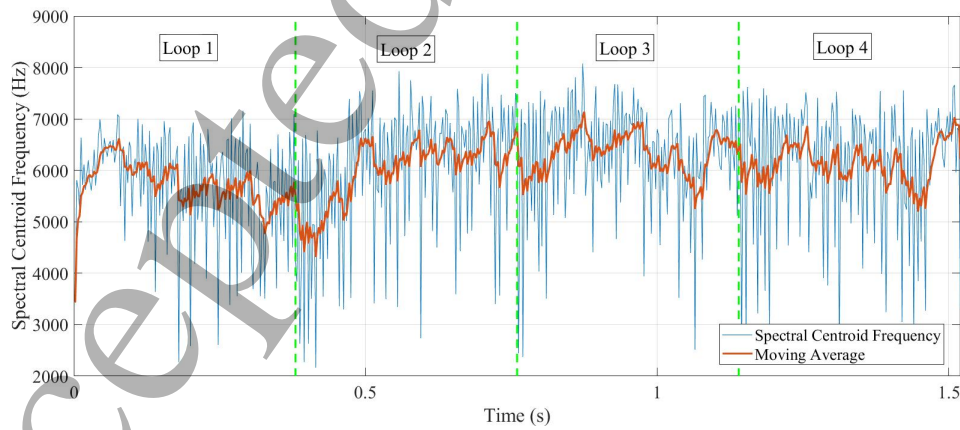
16 Figure 8 depicts the extracted trend of spectral centroid frequency from the signals of all  
17 experiments. In all instances with various process parameter configurations, it was discovered that  
18 the signal was quite intense at a bandwidth close to 6 kHz. In addition, the trend was nearly  
19 constant throughout the entire procedure. As shown in Figure 9, the roll off frequency was  
20 discovered to be approximately 10 kHz. Interestingly, the trend was also similar to the sound  
21 spectral centroid, whereas the value was almost constant. This finding indicates that there was no  
22 significant relationship between the frequency and amplitude behaviour of sound based on the  
23 sound frequency trend. Klein et. In their study, al [14] concluded that the frequency affects only  
24 the mode of plume ejection from the keyhole, but not the amplitude behaviour of the emitted sound.  
25 Instead, the sound amplitude was significantly affected by the quantity of ablated material ejected  
26 from the laser spot keyhole.  
27  
28  
29  
30  
31  
32  
33  
34  
35  
36  
37  
38  
39  
40  
41  
42  
43  
44  
45  
46  
47  
48  
49  
50  
51  
52  
53  
54  
55  
56  
57  
58  
59  
60



(a)

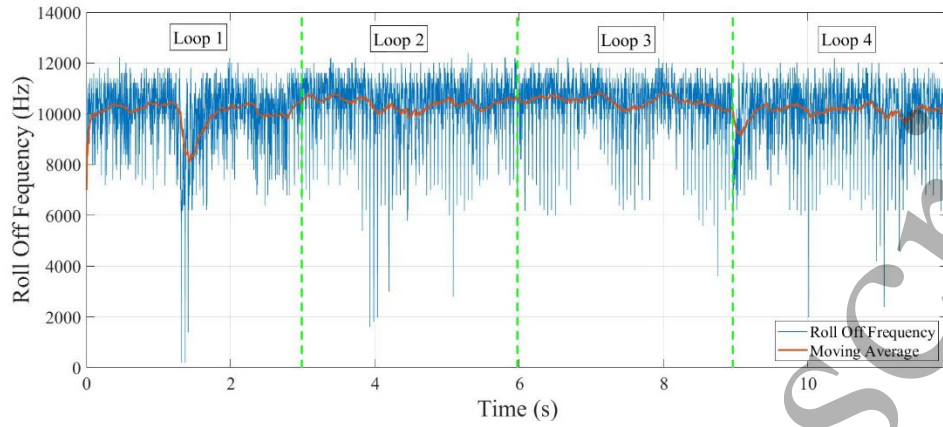


(b)

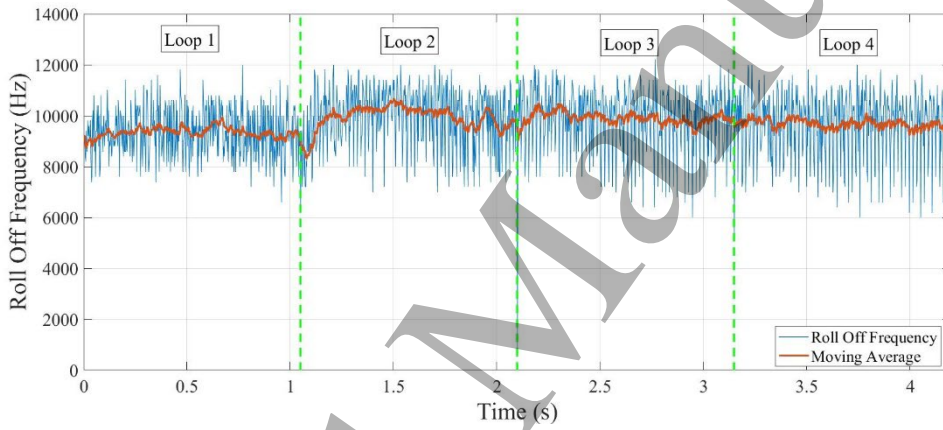


(c)

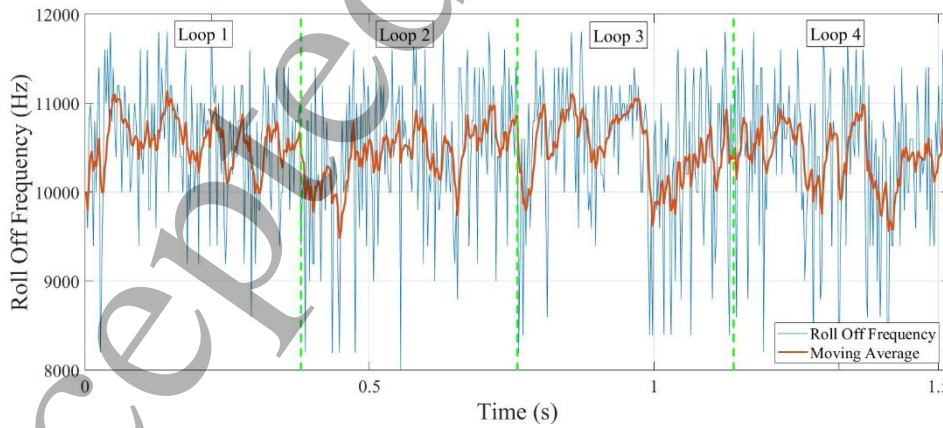
Figure 8 Spectral Centroid Frequency of the acoustic sound acquired during the process with the speed of (a) 100 mm/s (b) 300 mm/s (c) 1000 mm/s



(a)



(b)



(c)

Figure 9 Roll off Frequency of the sound during the process with the speed of (a) 100 mm/s (b) 300 mm/s (c) 1000 mm/s



Even though the active frequency was found to be unrelated to the cleaning status, the amplitudes or energies of these bands appear to provide crucial information regarding the amount of corroded substrate ablated during the cleaning process. This was evident as depicted in mel spectrogram plot in Figure 10. Referring to the diagram, it was found that the spectrogram energy was highest at the spectral centroid frequency, which was 6 kHz, in all instances. As shown in Figure 10(a) and (b) for the mel spectrogram, the power spectrum near 6 kHz was quite intensive when the ablated corroded substrate was dominant. The spectrum energy was discovered to be stable as the procedure continued. As shown in Figure 10(c), the spectrum energy was intense throughout the entire process when the scanning speed was 1000 mm/s. Aligned with the discussed results from Figure 7(c), this occurred because the corroded substrate persisted until the final loop of the process.

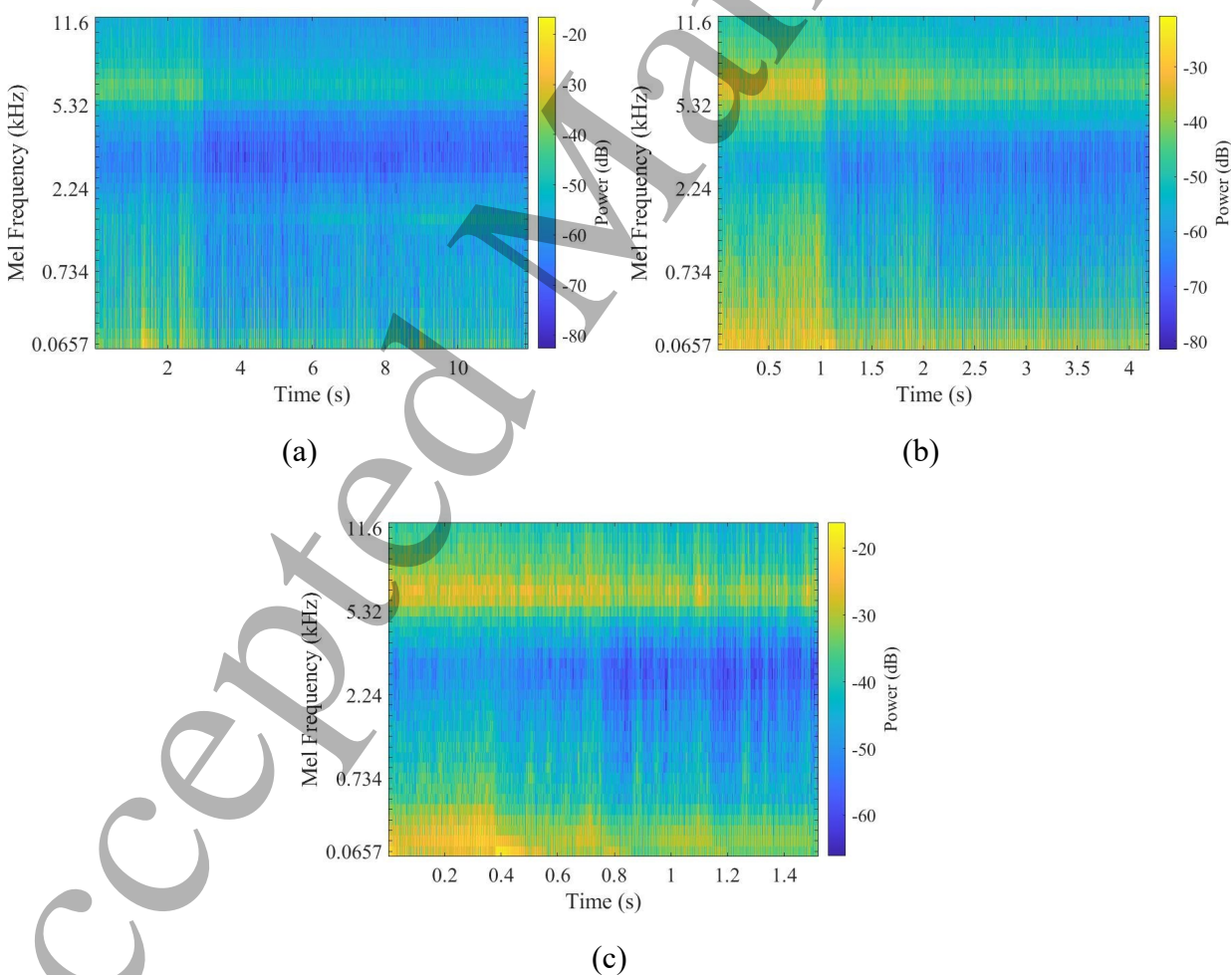
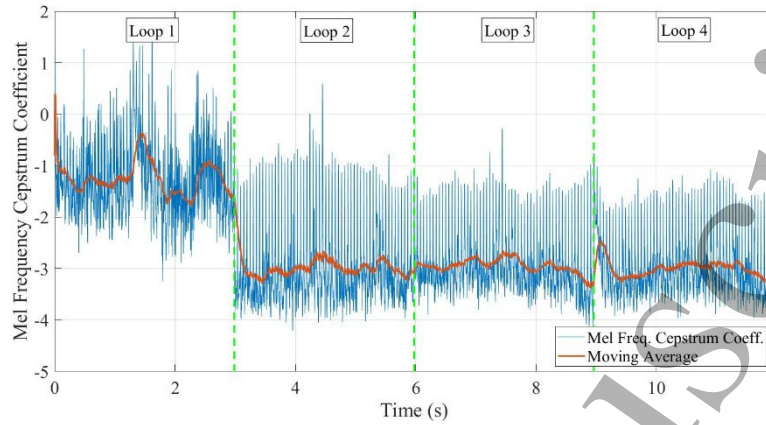
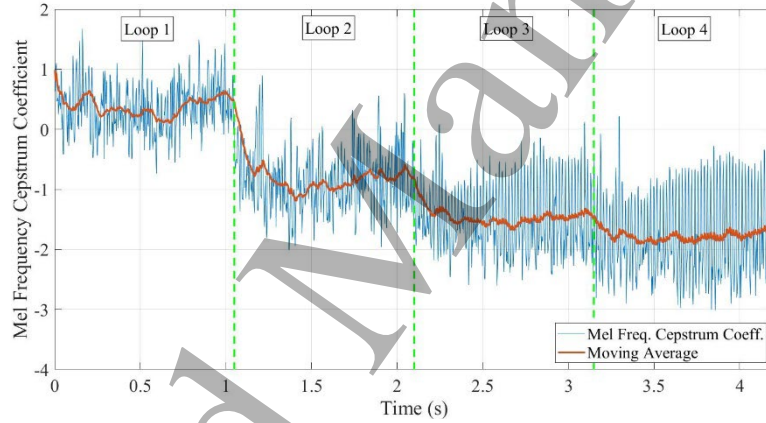


Figure 10 Mel Spectrogram of the sound during the process with the speed of (a) 100 mm/s (b) 300 mm/s (c) 1000 mm/s

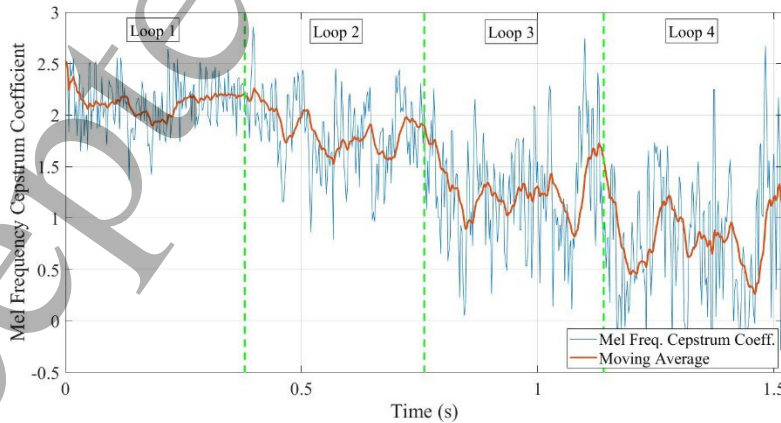
*Indication of the Cleaning Status during laser cleaning process from MFCC and Spectral Flux*



(a)



(b)



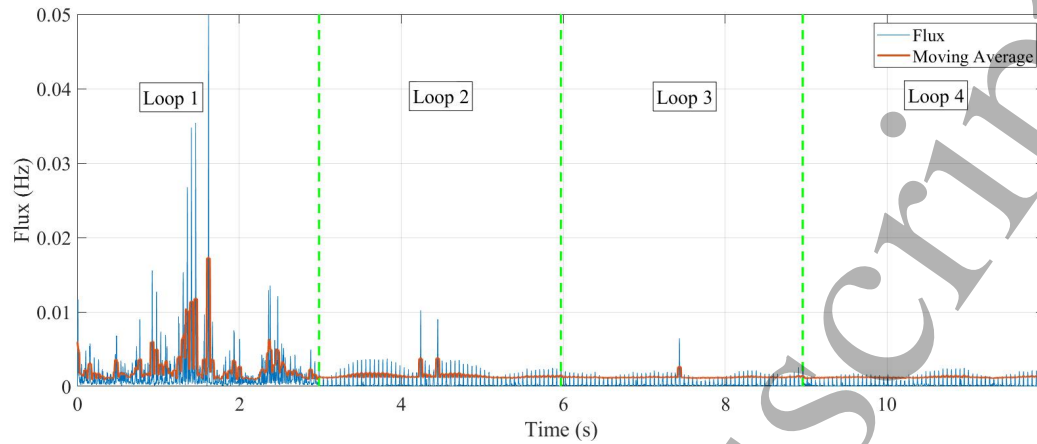
(c)

Figure 11 MFCC of the sound during the process with the speed of (a) 100 mm/s (b) 300 mm/s (c) 1000 mm/s

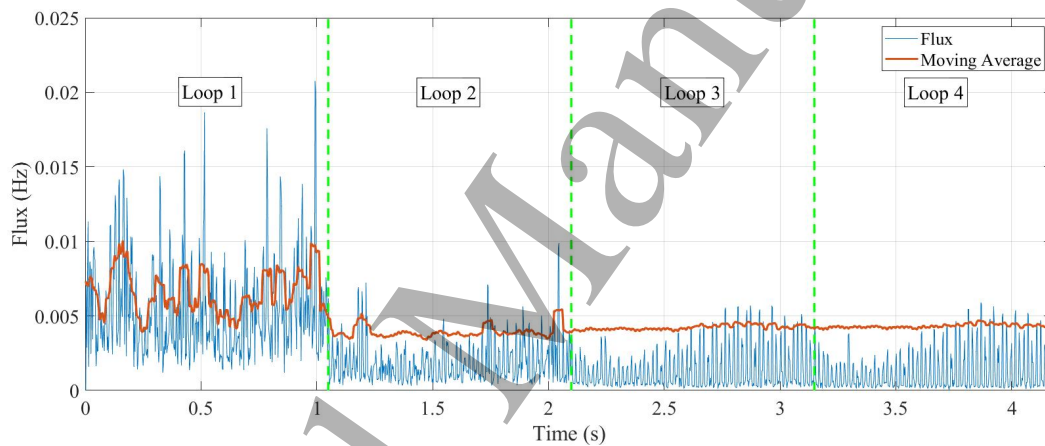
1  
2  
3  
4  
5 As stated in the previous section, the quantity of ablated corroded substrate had no effect on the  
6 signal frequency. However, the other characteristic of the signal might have a significant  
7 relationship with this phenomenon. Figure 11 depicts the extraction of the MFCC from the mel  
8 frequency spectrums for the purpose of gaining a comprehensive understanding of the laser  
9 cleaning process's trend and completion point of the corroded substrate removal. Figure 11(a)  
10 demonstrates that the MFCC decreases marginally to 2.95 seconds, for the process with the  
11 scanning speed of 100 mm/s. The value scarcely changed as the process continued until 5.9  
12 seconds, when it began to decrease. As the cleaning procedure progressed, the value was  
13 approximately maintained. Figure 11(b) reveals that, for 300 mm/s scanning speed, the average  
14 value of MFCC appears to decrease as the number of loops increases. Similar trends were also  
15 observed for laser scanning speeds of 1000 mm/s.

16  
17  
18  
19  
20  
21  
22  
23  
24  
25 As shown in Table 2, the corroded layer was effectively removed upon completion of the first  
26 process loop during the cleaning process with a speed of 100 mm/s. The high value of MFCC  
27 recorded in the first 2.95 seconds may be explained by the quantity of the corroded substrate that  
28 was ablated. Meanwhile, the cleaning process was completed during the second loop for the 300  
29 mm/s procedure. During the second cycle, the MFCC was unusually high despite the trend being  
30 significantly lower than in the first loop. This had made it challenging to use the MFCC as an  
31 indicator of laser cleaning process completion. The trend of results in Figure 11 suggested that the  
32 larger MFCC value could substantially indicate the presence of the ablation of the corroded  
33 substrate. However, it does not provide a distinct indication of the initiation of the engraving effect.

34  
35  
36  
37  
38  
39  
40  
41 Numerous earlier studies [9, 10, 13] demonstrated that during laser engraving or texturing, the  
42 quantity of plasma plume ejected from the ablated surface generates pulsed sound signals. This  
43 was owing to the fact that laser processing was performed in pulse mode. Due to this, the sound  
44 signal should be characterized based on its pulse behavior in order to indicate the commencement  
45 of the engraving process following the removal of the corroded substrate. In this investigation,  
46 spectral flux was extracted from the signal to determine the pulse pattern's origin.  
47  
48  
49  
50  
51  
52  
53  
54  
55  
56  
57  
58  
59  
60



(a)



(b)

Figure 12 Flux of the sound during the process with the speed of (a) 100 mm/s (b) 300 mm/s (c) 1000 mm/s

Figure 12 depicts the trend of the spectral flux of the acquired sound signals at 100 mm/s and 300 mm/s. Due to the reason that the process with a scanning speed of 1000 mm/s was only concluded after the fourth loop, the trend of spectral flux from this experiment was omitted from Figure 12. Figure 12(a) show that the flux trend was incoherent for the first 2.95 s, which corresponds to the first process loop. From the second loop until the end of the procedure, the flux value appeared to be much more stable whereas the moving average value was approximately constant at  $1.1255 \times 10^{-3}$  Hz. Meanwhile, for the process with a speed of 300 mm/s depicted in Figure 12 (b), the moving average value of the flux peak was significantly less stable than during the first circle. In

1  
2  
3 this instance, the flux value becomes significantly more stable during the third process cycle. In  
4 comparison to the results presented in Table 2, the flux value was more stable in the location where  
5 the roughness ratio was greater than 7.33. These results demonstrate that the stability of the flux  
6 value indicates the start of the engraving effect as compared to the MFCC.  
7  
8  
9

## 10 11 12 13 **CONCLUSION**

14  
15 This research examined the relationship between laser scanning speed and the characteristics of  
16 recorded sound signals. Several essential points can be drawn from the findings. The results  
17 demonstrated that the Mel Frequency Cepstral Coefficient was indicative of the presence of  
18 corroded substrate ablation. Moreover, the spectral flux value provides information regarding the  
19 formation of engraving effect following the complete removal of the corroded substrate from the  
20 surface. In case of laser cleaning with speed of 100 mm/s and 300 mm/s, the moving average of  
21 the flux value were approximately constant at  $1.1255 \times 10^{-3}$  Hz and  $4.1363 \times 10^{-3}$  Hz respectively  
22 at the point engraving effect started to exist. Even though the value was not equal for both cases,  
23 the stable trend indicates the overexposed laser beam which result in engraving effect after the  
24 completion of laser cleaning process.  
25  
26  
27  
28  
29  
30  
31  
32

33 Without resorting to laser parameters, the acoustic signal may provide vital information about laser  
34 cleaning quality, according to these findings. The findings of this study suggest that, with the  
35 necessary modifications, the acoustic method could be used to monitor laser cleaning in real time  
36 throughout the entire process.  
37  
38  
39  
40  
41  
42

## 43 **ACKNOWLEDGEMENT**

44  
45 Authors would like to thank to the Joining, Welding, and Laser Research Group, Faculty of  
46 Mechanical & Automotive Engineering Technology, University Malaysia Pahang for the facilities,  
47 and University Malaysia Pahang for providing a funding under grant no PDU213002-3 for this  
48 project.  
49  
50  
51  
52  
53  
54  
55  
56  
57  
58  
59  
60



## REFERENCES

- [1] Klingenberg, M. L., Naguy, D. A., Naguy, T. A., Straw, R. J., Joseph, C., Mongelli, G. A., Nelson, G. C., Denny, S. L., & Arthur, J. J. (2007). Transitioning laser technology to support air force depot transformation needs. *Surface and Coatings Technology*, 202(1), 45–57. <https://doi.org/10.1016/J.SURFCOAT.2007.04.056>
- [2] Zhang, P., Li, Z., Liu, H., Zhang, Y., Li, H., Shi, C., Liu, P., & Yan, D. (2022). Recent progress on the microstructure and properties of high entropy alloy coatings prepared by laser processing technology: A review. *Journal of Manufacturing Processes*, 76, 397–411. <https://doi.org/10.1016/J.JMAPRO.2022.02.006>
- [3] Wang, W., Sun, L., Lu, Y., Qi, L., Wang, W., & Qiao, H. (2022). Laser induced breakdown spectroscopy online monitoring of laser cleaning quality on carbon fiber reinforced plastic. *Optics and Laser Technology*, 145. <https://doi.org/10.1016/J.OPTLASTEC.2021.107481>
- [4] Raza, M. S., Das, S. S., Tudu, P., & Saha, P. (2019). Excimer laser cleaning of black sulphur encrustation from silver surface. *Optics and Laser Technology*, 113, 95–103. <https://doi.org/10.1016/J.OPTLASTEC.2018.12.012>
- [5] Xie, X., Huang, Q., Long, J., Ren, Q., Hu, W., & Liu, S. (2020a). A new monitoring method for metal rust removal states in pulsed laser derusting via acoustic emission techniques. *Journal of Materials Processing Technology*, 275, 116321. <https://doi.org/10.1016/J.JMATPROTEC.2019.116321>
- [6] Lee, J. M., & Watkins, K. G. (2000). In-process monitoring techniques for laser cleaning. *Optics and Lasers in Engineering*, 34(4–6), 429–442. [https://doi.org/10.1016/S0143-8166\(00\)00073-7](https://doi.org/10.1016/S0143-8166(00)00073-7)
- [7] Iwanicka, M., Moretti, P., van Oudheusden, S., Sylwestrzak, M., Cartechini, L., van den Berg, K. J., Targowski, P., & Miliani, C. (2018). Complementary use of Optical Coherence Tomography (OCT) and Reflection FTIR spectroscopy for in-situ non-invasive monitoring of varnish removal from easel paintings. *Microchemical Journal*, 138, 7–18. <https://doi.org/10.1016/J.MICROC.2017.12.016>
- [8] Tserevelakis, G. J., Pozo-Antonio, J. S., Siozos, P., Rivas, T., Pouli, P., & Zacharakis, G. (2019). On-line photoacoustic monitoring of laser cleaning on stone: Evaluation of cleaning effectiveness and detection of potential damage to the substrate. *Journal of Cultural Heritage*, 35, 108–115. <https://doi.org/10.1016/J.CULHER.2018.05.014>
- [9] Huang, F., Lei, M., Wang, J., Chen, D., Gao, T., & Wang, X. (2019). Sound waves generated by nanosecond and femtosecond laser ablation on different metals. *Optik*, 178, 1131–1136.
- [10] Kradolfer, S., Heutschi, K., Koch, J., & Günther, D. (2021). Tracking mass removal of portable laser ablation sampling by its acoustic response. *Spectrochimica Acta Part B: Atomic Spectroscopy*, 179, 106118.
- [11] Ayvaz, U., GÜRÜLER, H., Khan, F., Ahmed, N., Whangbo, T., & Bobomirzaevich, A. A., (2022). Automatic Speaker Recognition Using Mel-Frequency Cepstral Coefficients

1  
2  
3 Through Machine Learning. CMC-COMPUTERS MATERIALS & CONTINUA, vol.71,  
4 no.3, 5511-5521.  
5

- 6 [12] Zhang, G., Hua, X., Huang, Y., Zhang, Y., Li, F., Shen, C., & Cheng, J. (2020).  
7 Investigation on mechanism of oxide removal and plasma behavior during laser cleaning  
8 on aluminum alloy. Applied Surface Science, 506, 144666.  
9
- 10 [13] Stauter, C., Gérard, P., Fontaine, J., & Engel, T. (1997). Laser ablation acoustical  
11 monitoring. Applied surface science, 109, 174-178.  
12
- 13 [14] Klein, T., Vicanek, M., Kroos, J., Decker, I., & Simon, G. (1994). Oscillations of the  
14 keyhole in penetration laser beam welding. Journal of Physics D: Applied Physics, 27(10),  
15 2023.  
16  
17  
18  
19  
20  
21  
22  
23  
24  
25  
26  
27  
28  
29  
30  
31  
32  
33  
34  
35  
36  
37  
38  
39  
40  
41  
42  
43  
44  
45  
46  
47  
48  
49  
50  
51  
52  
53  
54  
55  
56  
57  
58  
59  
60